

Age dependent 3-1) Magnetic modeling of the North Pacific and North Atlantic oceanic crust at intermediate Wavelengths

Gonzalo A. Yañez

Servicio Nacional de Geología y Minería, Santa María 014, Santiago, (Wile

John L. LaBrecque¹

Jet Propulsion Laboratory, Pasadena, California, USA

Abstract. Three-dimensional magnetic modeling of the North Atlantic and Northeast Pacific is performed at intermediate wavelengths using three models for the acquisition of a natural remanent magnetization. It is shown that a remanent magnetization which is dependent on the crustal age is the dominant source for the intermediate wavelength pattern in both basins. However, a pure thermo-remanent magnetization of layer 2 alone is insufficient to model the intensity and shape of the observed magnetic anomalies at satellite altitude. We conclude that the best fitting magnetization model for both basins, is a combination of a chemical remanent magnetization in the altered upper crust and a thermoviscous remanent magnetization of the slowly cooling lower crust and upper mantle. The North Pacific requires a bulk magnetization which is 50% higher than that of the North Atlantic in order to fit the Magsat field. Geological processes associated with a faster spreading rate such as a faster hydrothermal alteration and the growth of a thicker gabbro layer at the expense of a weakly magnetized sheeted dike layer arc plausible explanations for the higher North Pacific magnetization. The lineated positive magnetic anomaly observed over the North Atlantic spreading center is not well reproduced by our models. This anomaly is likely due to a highly magnetized body along or in the vicinity of the spreading center. This highly magnetic body could be an unstable serpentinized lens of crustal material younger than 20 m.y. which develops within the zone cooled by hydrothermal circulation.

Introduction

The *Vine and Matthews* [1963] hypothesis defines a relationship between the magnetic reversal time scale and the age of the oceanic crust and is a cornerstone of plate tectonic theory. The hypothesis states that the oceanic crust acquires a natural remanent magnetization (NRM) in the form of thermal remanent magnetization (TRM) at the time of magmatic emplacement and cooling at the spreading axis. Although the hypothesis has been extremely successful in the study of plate tectonics, this simple mechanism cannot explain some characteristics of sea floor spreading magnetic anomalies nor the magnetization of dredged oceanic crustal samples.

For example, *Cande* [1976] discusses why shape asymmetry or skewness in the magnetic sea floor spreading anomaly pattern exhibits an anomalous component which cannot be explained by paleomagnetic pole positions. One notable feature of anomalous skewness is that it varies for individual magnetic anomalies. Various models were proposed to explain the anomalous skewness component including a diffuse boundary between uniformly magnetized bodies within layer 2A, undetected reversal events, and sloping boundaries in a magnetized gabbroic layer.

Systematic variations in magnetization intensity with respect to crustal age have been well documented. Both magnetic anomaly inversions and direct sampling of the sea floor

show that the upper crustal magnetization decays by an order of magnitude during the first 20 my. of crustal evolution [Irving *et al.*, 1970; Weissel and Hayes, 1972; Atwater and Mudie, 1973; Macdonald, 1977; Johnson and Atwater, 1977; Tivey and Johnson, 1987]. The NKM compilations of the Deep Sea Drilling Project (DSDP) dataset made by Bleil and Petersen [1983] display a consistent enhancement of NRM during the Long Cretaceous Normal (84-118 my.), in good agreement with the high amplitude quasi-lineated magnetic anomalies observed over the Cretaceous Quiet Zones (KQZ) of the North and South Atlantic [e.g., Labrecque and Rabinowitz, 1977; Vogt and Einwich, 1979; Labrecque and Raymond, 1985; Vogt, 1986].

The increased intensity of KQZ magnetization has been explained by at least four different mechanisms: (1) Main Field; an increase in the geomagnetic field intensity as a consequence of invigorated core convection and destruction of the D" layer [Pal and Roberts, 1988]. (2) Induction anomalies associated with the topography of the Curie isotherm [Cohen and Achache, 1990]. (3) CRM (chemical remanent magnetization): The growth of a time-dependent secondary magnetization in the upper crust [Raymond and Labrecque, 1987]. (4) TVRM (thermo-viscous remanent magnetization): The time-dependent acquisition of NRM as a result of lithospheric cooling through the spectrum of blocking temperatures appropriate for oceanic lithologies [Arkani-Hamed, 1989].

The generation of long period variations in the main field intensity is a complex theoretical problem of core magnetohydrodynamics [Merrill and McElhinny, 1983] that may be controlled by the magnetic Reynolds number, R . An increase in R favors stronger core convection and a stronger dipole field according to Pal and Roberts [1988]. They suggest that increased core convection generated a greater field intensity during the Cretaceous Long Normal and cite as evidence geomagnetic paleo-intensity measurements in igneous samples and paleo-heat flow estimations. The increase in heat flow is associated with the thermal disintegration of the D" layer (mantle plumes) due to the strong core convection.

Paleomagnetic evidence for an enhanced main field is controversial (e. g., see Merrill and McElhinny [1983] for a thorough discussion on the reliability of paleo-intensity measurements), moreover such a mechanism neither predicts the observed anomalous skewness in sea floor anomalies nor does it explain the slow decay of magnetization away from the spreading axis.

Fluctuations in the Curie isotherm surface have been suggested as a source mechanism for the Magsat field. Mayhew [1985] has inferred Curie isotherm depths from an inversion of the Magsat field for the western continental U.S. Labrecque and Raymond [1985] show a negative correlation between the Magsat field and the Curie isotherm depth over the North Atlantic spreading center. Cohen and Achache [1990] present an interesting positive correlation between magnetic and geoid anomalies in the North Pacific which may point to undulations in the Curie isotherm or variations in crustal thickness as a source mechanism for the intermediate wavelength field in this region. Because this proposed source layer is at depths of several tens of kilometers and may be

associated with subtle changes in the surface morphology of both the crust and the geotherm, better seismic and heat flow measurements could provide the data needed to verify this model.

Arkani-Hamed [1989] and *Raymond and LaBrecque [1987]* have shown that the TVRM and CRM models can reproduce the enhancement in the bulk crustal magnetization observed for oceanic crust of Cretaceous age as well as other aspects of the oceanic crustal magnetization. The simplicity of the models and their dependence on the geological processes associated with the evolution of the oceanic crust provide strong impetus to further test the validity of these models.

In this paper we perform 3-D modeling of the North Atlantic and North Pacific basins assuming these long term magnetic acquisition mechanisms. We will not invoke modulations in paleo-field intensity or discrete magnetic sources within the lower crust and upper mantle. We have chosen the North Atlantic and Northeast Pacific ocean basins because they may be considered end members in a spectrum of possible models. A large scale test of the NRM field over these basins was conducted by both *Cohen and Achache [1994]* and *Toft and Arkani-Hamed [1992]*. In this study we will develop a high resolution kinematic acquisition model to simulate the acquisition of magnetization by the aging oceanic lithosphere. We believe the results will provide more insight into the magnetization distribution of the oceanic crust. *Cohen and Achache [1994]* did not utilize an age dependent magnetization model which we believe is critical to defining the proper magnetization model for oceanic crust.

The North Atlantic (Figure 1) is characterized by a slow, spreading rate since its opening in the Middle Jurassic (~ 2 cm/yr, *Klitgord and Schouten [1989]*), a small N-S component of displacement, and a simple 2-D magnetization pattern (Figure 1 a). The sea floor spreading magnetic anomalies of intermediate wavelength form a nearly linear NNE trending pattern which extends from the ridge axis to the African and North American continental margins. Because of the simplicity of the source pattern, age-dependent 2-D forward magnetic models were applied to the region by *LaBrecque and Raymond [1985]*, *Raymond and LaBrecque [1987]* and *Arkani-Hamed [1989]*. Equivalent layer inversion schemes have also been applied to the North Atlantic by *Hayling and Harrison [1986]* and *Arkani-Hamed and Strangway [1985]*. All of these studies showed enhanced magnetization within the KQZ. *Hayling and Harrison [1986]* concluded that the magnetic lows observed along the older flanks of the North Atlantic KQZ are related to undulations in the crustal geotherm induced by sediment loading.

On the other hand, the North Pacific (Figure 2) was formed at a relatively high spreading rate and underwent a large northward displacement with respect to the geomagnetic field [*Engelbreton et al., 1985*]. Therefore the NRM is a function of the latitude of crustal emplacement and the path of the Pacific plate migration. The North Pacific magnetic anomaly pattern is also complicated by large age of first across fracture zones which requires a 3-D modeling approach.

Analysis of the intermediate wavelength component over the North Pacific has previously been restricted to two

dimensional profiles. *Harrison and Carle [1981]* concluded from the spectral analysis of a north-south profile along 210°E that deep mantle or highly magnetized oceanic crustal sources contributed to the intermediate wavelength magnetic anomaly pattern. However, *Shure and Parker [1981]* criticized the spectral analysis of single profiles on the basis of strike aliasing due to an improperly sampled two dimensional field, which would leak power from shorter wavelengths into the intermediate wavelength band. *Labrecque et al. [1985]*, showed that a gridded compilation of all sea surface data in the region filtered at intermediate wavelengths ($300 < \lambda < 3000$ km) could reproduce significant component anomalies of the Magsat field. Using forward modeling, *Labrecque et al. [1985]* also showed that the E-W anomalies of the Northeast Pacific (Figure 2c) are spatially related to the fracture zone pattern and could be modeled by the juxtaposition of normal and reversed magnetization across the fracture zones.

Theory and Methodology

We have considered three different models for the age dependent NRM: (1) a pure TRM - which is basically the Vine and Matthews hypothesis, (2) time-dependent CRM - the acquisition of a secondary magnetization in the upper crust [*Raymond and Labrecque, 1987*], and (3) time-dependent TVRM the viscous remanent magnetization model of *Arkani-Hamed [1989]*. The models are first applied to the North Atlantic where *Raymond and Labrecque [1987]* and *Arkani-Hamed [1989]* have studied two dimensional source distributions.

Magnetization Models

TRM

A pure TRM magnetization $\vec{M}_{TRM}(\phi_t, \theta_t, T)$ is a function of the geomagnetic field direction and the intensity at the time of cooling and the demagnetization with time:

$$\vec{M}_{TRM}(\phi_t, \theta_t, T) = \vec{M}(\phi_t) [\alpha, \beta, e^{-(T-t)/\lambda_T}] \quad (1)$$

where

T mean age of the crustal grid element (m.y.)

t geological time (m.y.)

ϕ_t, θ_t latitude and longitude coordinates at time t

λ_T time constant of TRM decay

β intensity component of transient TRM

α intensity component of fixed TRM

(*Raymond and Labrecque [1987]* found that the best fit of the demagnetization curve is obtained with $\alpha = 1/6$; $\beta = 5/6$ and $\lambda_T = 5$ my.)

$\vec{M}[\phi_t]$ magnetization vector at time t and latitude ϕ_t .

The magnetization vector $\vec{M}[\phi_t]$ is computed under the assumption of an axial dipole field whose intensity and direction is defined by [*Merrill and McElhinny, 1983*]:

$$|F_t| = F_0 (1 + 3 \cos^2 \phi_t)^{1/2} \quad (2)$$

$$\tan I_t = 2 \cot \phi_t$$

where

- F_0 magnetic field at the equator (0.33 Oe)
 I_t magnetic inclination (axial dipole approximation).

Then, the magnetization vector $\vec{M}[\phi_t]$ is computed as:

$$\vec{M}[\phi_t] = M \hat{M} \quad (3)$$

ii.) If e

- M equatorial normalized magnetization
 (e.g., 10 A/m)
 $= \|\mathbf{t}\| K R_f(t)$
 K magnetic susceptibility

- \hat{M} unitary vector of magnetic direction
 $= \{l_t \hat{x} + m_t \hat{y} + n_t \hat{z}\}$

- l_t, m_t, n_t direction cosines expressing the direction of the paleomagnetic field with respect to the crustal element at time t .

The reversal time scale $R_f(t)$ is a moving average of the true geomagnetic reversal time scale $R(t)$. The moving average reduces age aliasing within the crustal grid elements.

$$R_f(t) = \frac{(m+1)R(t) + \sum_{i=1}^m (m-i+1)(R(t+i\Delta t) + R(t-i\Delta t))}{(m+1)^2} \quad (4)$$

where

- $R(t)$ Geomagnetic Reversal Time Scale
 (1: normal, -1: reversed)
 Δt = 0.1 m.y.
 m = 5 (Pacific); 7 (Atlantic). The larger window in the Atlantic is due to its slower sea floor spreading rate.

CRM

The CRM model is a generalization of Raymond and LaBrecque (1987) in which the decay of a primary TRM is proportional to the growth of a secondary magnetization in the form of a CRM in the direction of the ambient field at the time of the chemical reaction. This chemical reaction, one form of which may be accomplished by the alteration of stoichiometric titanomagnetite to titanomaghemite followed by its phase splitting into Fe-rich titanomagnetite and titanilmenite, is assumed to continue for several million years within the crustal layer. Hydrothermal circulation may be the key element for this crustal oxidation because the intensity estimates of hydrothermal circulation with 111181 age resemble those of TRM decay on the spreading center flanks.

The growth of this secondary NKM is assumed to be the product of a first order chemical reaction [Raymond and LaBrecque, 1987]. The rate of a first order chemical reaction [A \rightarrow B] can be expressed as [Lasaga, 1981]:

$$\frac{dA}{dt} = -\frac{A}{\lambda_c} \quad (5)$$

which means that the reaction rate is proportional to the amount of reactive A present at any time. A can be associated with the unaltered titanomagnetite minerals whereas B is the alteration product. In this system a fraction P of the total amount of fresh material A_0 is available for the chemical reaction. Given this initial condition, the product B at a given time can be estimated by solving equation (5) and by assuming a closed system:

$$B = PA_0 - PA = PA_0(1 - e^{-t/\lambda_c}) \quad (6)$$

The growth of a secondary magnetization M and the product B must be linked in some way. Assuming that they are linearly related, then:

$$M = \gamma B = \gamma PA_0(1 - e^{-t/\lambda_c}) = PM_0(1 - e^{-t/\lambda_c}) \quad (7)$$

where

γ is the constant of proportionality ;
 M_0 the original bulk magnetization of the reactive A_0 .

The secondary magnetization is acquired in the direction of the ambient field at the time of the chemical reaction, therefore M in equation (7) becomes a vectorial magnitude that has to be integrated from the time of formation to the present in order to get the total NRM in the form CRM:

$$M_{CRM}(\phi_t, \theta_t, T) = M_{TRM}(\phi_t, \theta_t, T) + M_0 P \Delta t / \lambda_c \sum_{t=0}^T \hat{M}(\phi_t) e^{-(T-t)/\lambda_c} \quad (8)$$

where

t time increment
 P partition of the original magnetization (e.g., 0.66)
 λ_c time constant of CRM growth.

The first term on the right hand side is the pure TRM of Equation (1), the second term accounts for the growth of a secondary magnetization which is a function of the polarity, intensity and direction of the main field, time, paleo-latitude and orientation of the block. The exponential function modulates the magnetic acquisition. The fastest growth in CRM is achieved at the time of emplacement or $t = 0$. The acquisition of CRM reaches a saturation level with a time constant λ_c .

It is thought that the secondary magnetization is acquired at expense of the demagnetization of the original TRM, however the rate of this chemical reaction is uncertain. In our models we adopt $\lambda_c = \lambda_T$ as a first approximation, which means that the demagnetization-magnetization path is treated as a single geochemical reaction. If the main field direction changes continually, the net effect of the secondary magnetization tends to zero. On the other hand, during a long period of

constant polarity, the acquired CRM will dominate the bulk crustal magnetization.

Although there is significant evidence for low temperature alteration of magnetic minerals within the oceanic layer, the influence of low temperature alteration on the bulk magnetization remains unresolved. *Hall et al. [1986]*, *Hall et al. [1987]*, and *Hall and Fisher [1987]* report strong evidence of hydrothermal alteration throughout the extrusive and sheeted dike complex of the Troodos ophiolite complex. The evidence for hydrothermal alteration in the sheeted dike complex is accompanied by abundant secondary magnetite which diminishes towards the lower plutonic members. *Kelso et al. [1991]* have shown that low temperature alteration of synthetic titanomagnetite result in the growth of CRM in the direction of the ambient magnetic field and is unaffected by the preexisting TRM. However, *Beske-Diehl [1990]* reports no evidence of CRM in an extensive and careful study of DSDP and dredge samples from a variety of upper crustal locations and ages. *Smith and Banerjee [1986]* and *Pariso and Johnson [1991]* report that a strong secondary magnetization resulting from hydrothermal alteration contributes to the magnetization at ODP site 504B throughout the presently sampled section. As with the Troodos ophiolite, evidence for hydrothermal alteration diminishes toward the deeper sections of the sheeted dike complex (layer 2C).

TVRM

The TVRM model, proposed by *Arkani-Hamed [1989]*, generates sloping boundaries for the lithospheric magnetization contrasts. These surfaces are determined by the downward migration of the isothermal surfaces during the cooling of the lithosphere. The alternation of magnetic polarities during crustal cooling within a vertical lithospheric column results in a set of sub-blocks magnetized in alternating directions. If the polarity of the geomagnetic field is rapidly varying during the cooling of the lithosphere, then the bulk magnetization of the vertical column is reduced considerably. During a period of no geomagnetic reversals (e.g., Cretaceous Long Normal) the vertical column is magnetized in a single direction, and exhibits a strong magnetic anomaly.

The TVRM model assigns a significant viscous magnetization to the entire lithosphere when it cools below the Curie point of the magnetite (580 °C). A stable remanent magnetization is acquired after cooling below a nominal blocking temperature (400 °C). In this model the extrusive and intrusive basalt layer (layers 2A, 2B, and 2C) rapidly acquire their remanent magnetization. While the gabbroic layer (layers 3A and 3B) and the upper mantle (>8 km) lock in a remanent magnetization following a conductive cooling period which increases with depth. Therefore, lithospheric magnetization is acquired to depths of approximately 40 km long after the emplacement and magnetization of the upper crustal sections.

A uniform magnetization intensity is assigned to all sources below the sheeted dike complex (layer 2A). We have used values 1.6 A/m for the North Atlantic Basin modeling, while the Pacific model values are 50% higher (2.4 A/m). The 1.6 A/m value is in accordance with the most recently measured

values for insitu gabbros at ODP site 735B [Kikawa and Paraiso, 1991] but higher than some compilations such as Hayling and Harrison [1986] and Harrison [1987] who give values ranging from 0.6 to 1.3 A/m depending on the degree of serpentinization. Magnetization intensities for the mantle are more uncertain. Wasilewski *et al.* [1979] suggest that the mantle is nonmagnetic while Harrison [1987] suggests that tectonized and serpentinized mantle material may form a magnetized layer on the order of 5 A/m within the lower crust and upper mantle.

The TVRM magnetization of a vertical column of oceanic lithosphere is a function of the geomagnetic field direction at the time of cooling below its blocking temperature. The time dependent cooling of the ocean lithosphere is primarily achieved by thermal conduction. However, the upper 1.5 km of oceanic crust cools more quickly due to active hydrothermal circulation during the first 2.0 m.y. of crustal evolution. Therefore layer 2 is assumed to acquire its magnetization nearly instantaneously compared to that of the lower crust and upper mantle.

The thermal evolution of the oceanic lithosphere is approximated by a 2-D conduction cooling model [e.g., Parker and Oldenburg, 1973; McKenzie, 1967]. In this model the depth to a given blocking isotherm at time t after the cooling of the uppermost oceanic crust is

$$H_1 = \alpha_{\text{block}} \sqrt{T - t} \quad (9a)$$

H_1 represents the oceanic lithosphere section which has already acquired a remanent magnetization. The proportional factor α_{block} is a function of the blocking temperature used (e.g., $\alpha_{580^\circ\text{C}} = 4.3$, $\alpha_{400^\circ\text{C}} = 2.811$, $\alpha_{600^\circ\text{C}} = 1.4055$). After an interval of t million years, the magnetic layer increases by

$$\Delta H_1 = \alpha_{\text{block}} [\sqrt{T - t + \Delta t} - \sqrt{T - t}] \quad (9b)$$

while acquiring a NRM proportional to the ambient magnetic field at $\vec{M}[\phi_t]$ (equation 3). Thus, the bulk magnetization of the entire lithospheric section of crustal age T can be written approximately as:

$$\vec{M}_{\text{TVRM}}(\phi_t, \theta_t, T) = \vec{M}_{\text{TM}}(\phi_t, \theta_t, T) + \sum_{t=T-\tau}^T [\vec{M}(\phi_t) \Delta H_t] + \vec{M}(\phi_t) (\alpha_{\text{src}} - \alpha_{\text{m}}) F_1 \sqrt{T - t} \quad (10)$$

Where F_1 is the geometric factor which accounts for the distance from the source to the observation point.

$$F_1 = \frac{Z_0^2}{[Z_0^2 + H_1]^2} \quad (11)$$

If Z_0 , the altitude of observation, is much larger than the source thickness H_1 , then F_1 approaches 1. In practice, instead of using the approximate expression of \vec{M}_{TVRM} (equation (10)) we compute the effect of each crustal element.

The use of $\vec{M}_{TRM}(\phi, \theta, T)$, is a modification of the original formulation of *Arkani-Hamed* [1989], that allows for the observed demagnetization of the spreading center flanks. The summation of the second term starts at the time in which the top of the gabbro layer is cooled below its blocking temperature (~2 m.y.). The last term represents the viscous magnetization of a layer bounded by the blocking and Curie isotherms.

Comparing \vec{M}_{TVRM} and \vec{M}_{CRM} (equations (1) and (8) respectively), we have a common first term which is a TRM magnetization of the uppermost oceanic crust (layer 2A, 0.5-1.0 km). The second term represents a secondary magnetic acquisition through time. In both models the rate of growth of this secondary magnetic phase decreases in time, but not at the same rate.

Figure 3 illustrates the effect of the growth of the secondary phase in CRM and TVRM magnetization under a fixed magnetic field environment. The approximation of TVRM magnetization by an equivalent magnetic layer gives different responses at sea surface and satellite altitudes because of the geometrical factor F_r . At satellite altitude both models, CRM and TVRM, display a similar growth during the first 4 m.y. As time proceeds, the CRM model asymptotically reaches a maximum bulk magnetization within 10 m.y. while the TVRM model continues growing at a small but constant rate.

The distinctive pattern of these models is associated with the mechanisms of magnetic acquisition which are active in each case. The CRM is a product of a chemical reaction which decreases with time either because of the consumption of available material or by the change in the conditions which favor the reaction (e.g., decrease in hydrothermal circulation or temperature). The TVRM model depends on the cooling of the lithospheric plate which is an asymptotic process during the first 10 m.y. of the oceanic plate.

The growth rate of TVRM at the sea surface compared to the satellite altitude is much faster during the first 3-4 m.y. followed by a slower growth rate. This behavior is a consequence of the greater magnetization of the shallow (rapidly cooled) lithospheric magnetic sources with respect to the deeper (slowly cooled) sources.

Because of these differences in the acquisition of secondary remanence we would expect some discrepancies between CRM and TVRM models, both at 400 km and at the sea surface. The third term in the TVRM model (equation 10), represents the viscous component that could make a difference in models across large age offset fracture zones. In this case, the thickness of the viscous component will differ by a large amount across the fracture zone, particularly for young lithosphere.

Forward Modeling: Atlantic and Pacific Basins

Using the magnetic models of the previous section, a synthetic magnetic field is computed and then compared with the Magsat field produced by *Arkani-Hamed and Strangway* [1985] (Figures 1c, 2c) and sea surface data processed with an improved technique whose elements are described in *LaBrecque et al.* [1985].

In the Magsat field of *Arkani-Hamed and Strangway* [1985] the dawn and dusk data were processed separately and band-passed within a window of order $17 < n < 53$ prior to summing.

both data sets. The version of the Magsat field provided to us by Arkani-Hamed contains components to order 60 with significant energy to wavelengths of 650 km. Therefore to compare our model fields to the Magsat field we filtered all the anomaly fields to the same bandpass of 2000 to 650 km. The high pass filter cutoff of 2000 km insures that core field sources are reduced to negligible levels [Langel and Estes, 1982]. The low pass cutoff of 650 km may produce problems in that both Sailor et al. [1982] and Arkani-Hamed and Strangway [1985] report low inter-track coherences at wavelengths shorter than 800 km. However, a more restrictive low pass cutoff of 800 km applied to the Magsat field reduced anomaly levels by 50% without changing the general form of the anomaly field. Therefore, we have used a broader bandpass in the hope of optimizing anomaly resolution.

The magnetic source layer is divided into a 2-D grid whose elements are approximately 1 degree square. Although the low pass filter cutoff of 650 km can be satisfied using a 3 degree square grid element, a finer grid was utilized to prevent aliasing of magnetization distribution. A mean age is assigned to each element according to the world age compilation of Cande et al. [1989]. In general, we estimated the crustal age within the KQZ by linear interpolation. However, some areas of the Pacific region lack good age control because of a poor identification of either anomaly M0 or 34 (such as the KQZ between the Murray and Clarion fracture zones). As we will see later, the assumption of linear age gradients within the KQZ may require some modification.

Once the age grid is defined, each grid element is positioned with respect to the estimated axially oriented paleo-dipolar field for the time of crustal emplacement and subsequent cooling near the paleo-spreading center. We used the rotation poles of Engebretson et al. [1985] for the Pacific and Morgan [1981] for the Atlantic reconstructions, both of which assume a hotspot reference frame. Figures 1b and 2b show the paleo-latitude of each grid element at the time of emplacement within the Atlantic and Pacific basins respectively. The path of each grid element is calculated in steps of 1 million years (generally 0.1). At each step the magnetization is computed through the evaluation of the axial dipole magnetic field, the orientation of the block and the given magnetization model. Once the total magnetization distribution is determined, the magnetic anomaly field is computed either in the frequency domain [Battacharya, 1966] to enhance calculation time or in the space domain [Plouff, 1976] to enhance the resolution. The models are computed assuming a flat earth. Differences between spherical and flat earth modeling are less than 15% at satellite altitude [LaBrecque and Cande, 1984], but the advantages of computational efficiency outweigh the disadvantage of modeling inaccuracies.

The goal of the magnetic models described in the previous section is to reproduce the magnetic response of a homogeneous oceanic lithosphere. Magnetic anomalies associated with structural features, like the Hawaiian chain and the Mid-Pacific Seamounts produce significant anomalies at satellite altitude [e.g., LaBrecque and Cande, 1984; Fullerton et al., 1989; Bradley and Frey, 1988].

We have included in the computed synthetic fields, the source calculations for the Mid-Pacific and Hawaiian Seamounts to improve the comparison between model and observation. We have modeled the seamounts with a TRM magnetization acquired at the time of the seamount construction. The volumes of the seamount were determined by bathymetric contours and the seamount magnetization was set at 6 A/m for simplicity. Generally the correspondence was very good with the observed data. In particular the observed seafloor data (Figure 6a) clearly show the Hawaiian anomaly which is reproduced by our models (Figures 6c,d). Certainly more care could have been taken in modeling the seamounts given the extensive literature on the topic. However, the nature of this study did not warrant a more detailed approach.

Results

North Atlantic: Magsat Altitude of 400 km

The Magsat field over the North Atlantic basin is influenced by the continental magnetization at both flanks, as was first suggested by *Meyer et al.* [1985]. Therefore a good characterization of the oceanic crust magnetization is difficult in this basin. This contamination affected the analysis of *Labrecque and Raymond* [1985] and *Raymond and Labrecque* [1987]. To reduce the effect of the continental source distribution, the magnetic field produced by the equivalent source distribution of *Arkani-Hamed and Strangway* [1985] over the continents has been removed from the Magsat field. The removal of the estimated continental component reduces the amplitudes of some anomalies over the North Atlantic while leaving unaffected others such as the positive within the KQZ south of the Atlantis FZ on the western flank, its equivalent on the eastern side and the anomalies located between the KQZ and the center of the basin.

The models employ an average magnetization of 3.833 A/m (normalized to the equator) for an equivalent layer source thickness of 1.5 km, as required to fit the Mesozoic and Cenozoic sea floor spreading anomaly sequences in the North Atlantic [*Pitman and Talwani*, 1972] at the sea surface. An average magnetization of 3.833 A/m implies an initial spreading center magnetization of 20 A/m and 8.7 A/m in the TRM and CRM models respectively (with $\lambda_T = \lambda_C = 5$ my.). For the TVRM model, layer 2 is modeled with a TRM magnetization of 20 A/m and a layer 3 and upper mantle magnetization of 1.6 A/m, assuming a blocking temperature of 400 °C.

Figure 4 illustrates the forward magnetic modeling results. Figure 4b shows clearly that a pure TRM following the constraints of sea surface anomalies is not sufficient to model the satellite level anomalies within the KQZ south of the Atlantis FZ. Conversely, CRM and TVRM models (Figures 4c and 4d respectively) reproduce the observed anomalies and shapes within the KQZ to a reasonable degree.

Though we have attempted to remove the effect of the non-oceanic crustal magnetizations by including estimates of the continental susceptibility in our models, the desired effect apparently fell short of our goal. The remanent magnetization

models reproduce the observed Magsat field over the KQZs, but the anomalies over the eastern margin of North America, the Caribbean and the North Atlantic spreading center are not reproduced. It is likely that the mismatch could be due to an induced magnetization contrast as discussed by *Counil et al.* [1991]. Future studies should focus on further defining this effect and the resulting mismatch. The positive north-south anomaly associated with the ridge crest is far from the continental masses and the high geomagnetic reversal rate and thin lithosphere of the young oceanic crust suggests a source distribution other than remanent magnetization. *LaBrecque and Raymond* [1985] model the spreading center anomaly with a high susceptibility source which diminishes exponentially to 30% of the maximum value at 100 km from the spreading center.

A good candidate for a highly magnetized source at the spreading center is a partially serpentinized lower crust and upper mantle. *Shive et al.* [1988] report that at metamorphic grades below the amphibole facies, serpentinite remains the stable phase while higher grades of metamorphism tend to deserpentinize the rock. On the flanks of the spreading center, the degree of metamorphism is mainly controlled by the geothermal gradient. Strong hydrothermal circulation in the vicinity of the spreading center [Anderson, 1972] may keep the region cool enough to enable the growth of a stable serpentinized phase.

Anderson postulates that the decay in hydrothermal circulation away from the spreading axis heats the hydrous phase above the hydration-dehydration temperature of its constituent assemblage, providing a mechanism for the disintegration of the partially serpentinized layer. Therefore, the evolution of a hydrothermal circulation system can account for a lens of high susceptibility crust along the spreading center.

Northeast Pacific: Magsat Altitude of 400 km

The modeling of the Northeast Pacific region is complicated because of its large northward displacement since crustal formation. However, the reliability of the intermediate wavelength field is improved by the fact that the continental margin edge effects are located far away from the area of interest and there is no significant spreading system nearby.

Surface magnetization models for the North Pacific sea floor spreading pattern [Pitman et al., 1968] require a magnetization or equivalent thickness 50% greater than the values of the North Atlantic, which translates to a reference magnetization of 5.0 A/m normalized to the equator for a 1.5 km source thickness. As in the North Atlantic, the TRM field model (Figure 5b) amplitudes are less than 50% of the Magsat field, using an initial spreading center magnetization of 30 A/m. The long term magnetic acquisition models (CRM and TVRM, Figures 5c and 5d) reproduce the east-west trend in the KQZ and the NNW-SE pattern in the Cenozoic sequence with the appropriate amplitudes. Considering uncertainties associated with sources other than age related magnetizations, the uncertainty in the age of the western central Pacific, and the strong northward displacement of the Pacific plate during the Cenozoic, the 3-1) magnetic modeling of the Magsat field is surprisingly good.

The effect of anomalous skewness first observed in the North Atlantic is also observed in the North Pacific. In the TRM model (Figure 5b) the anomalies associated with the KQZ are shifted 2-3 degrees of longitude eastward of the Magsat field (Figure 5a). While the CRM and TVRM models (Figures 5c and 5d) properly reproduce the observed anomaly field.

As expected, there is a good correspondence between the CRM and TVRM anomaly fields since they both attempt to model the same observations using the geomagnetic field history. An obvious difference between the two models is the location of the maximum associated with the Murray Fracture Zone within the Pacific KQZ (25°N, 1650-145°W). The TVRM field anomaly is displaced 5 degrees to the south with respect to the Magsat field, while the CRM model reproduces the proper location and shape of the Magsat anomaly.

The oceanic crust between Murray and Molokai Fracture Zones is bounded by oceanic crust 10-15 m.y. older on both its northern and southern flanks (Figure 2a). Because of this age difference, along a meridional profile at 155°W, the inductively magnetized crust which lies between the 400°C blocking temperature isotherm and the Curie isotherm is 1.6 km thinner under the younger crust. The layer above the blocking temperature isotherm is also thinner and the skewing effect of this crustal magnetization is diminished. Therefore this region of mid-Cretaceous to Paleocene crust provides a good point of comparison between the CRM (which is independent of the lithospheric thermal state) and the TVRM III(1C).

The fit of our models is relatively poor in the area west of 165°W, in fact there appears to be nearly a negative correlation between our models and the observed field. This discrepancy can be attributed either to errors in the estimated age, or to a magnetic overprint associated with the Hawaiian Islands and the Mid-Pacific Seamounts. We have attempted to model the effect of both the Hawaiian and the Mid-Pacific Seamounts. The anomalies can be most easily observed in the TRM field at 155°W and 20°N and 160°W and 5°N respectively.

Errors in the basement age estimates could be attributed to the transition between the magnetic lineations of the Phoenix and Hawaiian M-sequence (seen along the western boundary of these maps) and the Mid-Cretaceous Quiet Zone. The transition between the three spreading systems is not clear and a major age discontinuity could exist within the region. This transition may have developed along a triple junction or as discrete spreading center jumps. Our confidence in the observed field developed through the match to the Mid-Cretaceous and Cenozoic Pacific magnetization distribution leads us to believe that the western Pacific mismatch is due to either age or structurally related magnetization anomalies in this region.

Discussion

Higher Magnetization in the Pacific with Respect to the Atlantic: A Spreading Rate Dependence?

W C . have shown that anomalies associated with the intermediate wavelength anomaly pattern over the Cretaceous and Cenozoic crust of the North Atlantic and North Pacific can be reproduced using an age dependent remanent magnetization source layer (CRM or TVRM). In order to match the Magsat field using the same source layer thickness, we found that the North Pacific requires a bulk magnetization which is 50% greater than that of the North Atlantic.

Considering the CRM model, the difference between the Atlantic and Pacific bulk magnetization can be explained by different rates and depth of penetration for the alteration reaction which generates the chemical remanence. This chemical reaction is controlled mainly by the pattern of hydrothermal circulation within the oceanic crust. The water flow through this medium is sensitive to local factors such as the sedimentary cover and porosity. The average sediment cover differs dramatically between the Pacific and Atlantic basins. In the Atlantic, the sediment thickness averages of 0.5-1.0 km between anomalies M0 and M34 [e.g. Tucholke and McCoy, 1986], whereas in the Pacific Basin the average sedimentary cover is on the order of 100 meters [Winterer, 1989].

If a thicker sedimentary cover inhibits the hydrothermal flow as suggested by Anderson *et al.* [1977], then we would expect more intense hydrothermal circulation during the early stages of crustal cooling in the Pacific. Heat flow measurements compiled by Anderson *et al.* [1977] are consistent with a much longer period of hydrothermal circulation in the Atlantic than in the Pacific. Therefore, if the initial crustal porosity is similar in both oceans [Carlson and Herrick, 1990], then the shorter period of hydrothermal activity in the Pacific is indicative of a more active initial circulation and a faster reduction in crustal porosity through the precipitation of secondary mineralization, perhaps favored by a higher temperature environment.

From the Arrhenius equation [Lasaga, 1981], the reaction rate $1/\lambda_c$ grows exponentially with an increment T in temperature. At high and intermediate rate spreading centers, high temperature (~300 °C) hydrothermal activity is commonly observed while these high temperatures are rarely observed at slow spreading rates [Macdonald, 1983]. This suggests a difference in hydrothermal circulation of about 50 °C [Anderson *et al.*, 1977] between fast and slow spreading systems.

The reaction rate is also controlled by the poorly known activation energy parameter. According to Lasaga [1981], the activation energy for most geochemical reactions is in the range of 10-20 Kcal/°K. If this range applies, the reaction rate in fast spreading regimes would be about 2 times the reaction rate in slow spreading regimes.

In the CRM model, a more intense hydrothermal circulation for a shorter duration would be characterized by a faster

reaction (smaller 2- 2-3 my.) implying sharper magnetic boundaries and stronger magnetic anomalies, characteristics that we find in the Pacific region.

The enhancement in bulk magnetization of the Pacific can be partially explained in terms of a spreading rate dependence of the oceanic crust structure. Seismic experiments [Vera *et al.*, 1990; White *et al.*, 1990] and thermal models [Kusznir, 1980], show that at slow spreading rates (e.g., the Atlantic) a thick sheeted dike layer (-2,-3 km) is developed at the expense of the gabbro layer. Conversely, in fast regimes the sheeted dike layer is reduced to the advantage of the gabbroic magma chamber residuum. We assigned the same magnetization values to both the sheeted dike and gabbroic layers. If the gabbroic layer were more magnetic than the development of a thicker gabbroic layer in the Pacific (a fast regime) could increase the bulk magnetization.

CRM v/s TVRM: A Comparison at the Pacific Sea Surface

We have shown that at high altitude both CRM and TVRM models reproduce the dominant features of the magnetic field at intermediate wave length, confirming the near equivalence of both models far from the magnetic source. A better way to test the validity of each model is to compare them at the sea surface where the resolution of the magnetic anomalies is enhanced. A highly magnetized thin source layer (CRM model) and a moderately magnetized thick source layer (TVRM model) have distinctive magnetic patterns at the sea surface.

The sea surface CRM and TVRM models for a smaller region between latitudes 10° to 30° N are presented in Figures 6c and 6d. In this case the magnetic field is computed using blocks of 12 minutes and filtered to a wider bandpass of 2000 to 350 km. The amplitudes and gradients of the synthetic magnetic field generated by the CRM model (Figure 6c) are greater than those of the TVRM model (Figure 6d) while the broad negative anomaly flanked by the Molokai and Clarion Fracture Zones is better developed in the TVRM field. These differences are the natural consequence of the source distribution. For an equivalent field at high altitude, a concentrated shallow source (CRM) produces sharp high intensity anomalies whereas a deep distributed source (TVRM) contributes more to the long, wavelength components (deeper sources).

Figure 6a displays a new sea surface compilation at the 2000 to 350 km bandpass following the technique of Labrecque *et al.* [1985]. The data in this compilation have been carefully edited for errors and external field effects have been removed. The data set is expanded over that available in the earlier 1985 compilation and better defines the regional anomalies. The highest data density is located around Hawaii where the low amplitude positive anomaly south and negative anomaly north of the island chain depends on the calculated effect of a TRM source within the island chain.

A comparison of the observed sea surface field to the CRM and TVRM fields yields interesting correlations and discrepancies. The anomaly gradients across the fracture zones or across the major seafloor spreading anomalies such as 34, display a stronger correlation to the CRM field. Conversely, the long wavelength components like the prominent negative

between the Murray and Clarion Fracture Zones is better represented in the TVRM field, suggesting that deep sources are likely in the region.

The strong broad negative anomaly west of anomaly 34 between the Clarion and Molokai Fracture Zones is very informative as to possible source distributions. In the TVRM field we see a negative westward sloping gradient which is the skewed contribution of the lower crust and upper mantle while the layer 2 contribution displays a relatively small unskewed gradient due to the weak magnetization of layer 2. The CRM field on the contrary displays a strong westward skewed gradient across anomaly 34 because the contribution is largely from nearby sources in the highly magnetized upper crust.

The observed field (Figure 6a) displays both a broad negative suggesting a strong contribution from the deeper crust while exhibiting the strong skewed gradient structure of the CRM field. It is difficult to ascertain from the available sea surface data which form of magnetization dominates but a strong deep mantle magnetization is a strong possibility in this region. Therefore, from the comparison at sea level, it appears that the oceanic magnetization structure is best modeled by a combination of the CRM and TVRM models.

For the TVRM model, the lower crust and upper mantle are likely to have a mean magnetization on the order of 2-3 A/m superimposed upon a slightly diminished CRM/TRM component from layer 2. More modeling of regions with large offset fracture zones and a more extensive compilation of the intermediate wavelength field need to be completed before a more definitive magnetization model can be proposed. Also more work should be addressed toward the appropriate values for the Grit isotherm and blocking temperatures applicable to the upper mantle. We have used values of 580°C for the mean Curie isotherm and 400°C for the mean blocking temperature. Variations in these parameters will influence the resulting TVRM anomaly field.

The sea surface compilation in Figure 6a shows that in addition to the modeled age dependent magnetizations, there appears to be other significant source mechanisms. The intermediate wavelength magnetic field is clearly an important data set with which to study the long term evolution of the ocean lithosphere.

Conclusions

1. Although a simple TRM of crustal layer 2 appears to model the general morphology of the observed intermediate wavelength magnetic anomaly fields of the Northeast Pacific and North Atlantic, it is insufficient to explain the intensities of these fields.

2. A combination of both CRM and TVRM magnetization models reproduce most of the features observed in the Magsat and sea surface fields at intermediate wavelengths over the Northeast Pacific and North Atlantic. CRM is the major component of magnetization for the upper crust (layer 2) while TVRM is the major component of magnetization for the lower crust (layer 3) and upper mantle.

3. The bulk magnetization of the Pacific is 50% greater than the Atlantic. This can be explained in terms of geological processes associated with the sea floor spreading environment.

4. The magnetic anomaly observed along the Atlantic spreading center may be due to a serpentinized layer within the lower crust and upper mantle. This transient strongly magnetized layer is unstable at high metamorphic grades, and therefore is continuously destroyed away from the spreading center.

Acknowledgments. We wish to thank Paul Wessel and Walter Smith for providing the GMI display software. This effort was supported by NSF Ocean Sciences Program grant OCE-90-13383, NASA Geodynamics and Geopotential Fields Programs under UPNS 465 and 579, the Chilean Servicio Nacional de Geología y Minería and Columbia University.

References

- Anderson, R. N., Petrologic significance of low heat flow on the flanks of slow-spreading mid-ocean ridges, *Geol. Soc. Amer. Bull.*, 83, 2947-2956, 1972.
- Anderson, R. N., M. G. Langseth, J. G. Sclater, The mechanism of heat transfer through the floor of the Indian Ocean, *J. Geophys. Res.*, 82, 3391-3409, 1977.
- Arkani-Hamed, J. and D. W. Strangway, Lateral variations of apparent magnetic susceptibility of lithosphere deduced from MAGSAT data, *J. Geophys. Res.*, 90, 2655-2664, 1985.
- Arkani-Hamed, J., Thermoviscous remnant magnetization of oceanic lithosphere inferred from its thermal evolution, *J. Geophys. Res.*, 94, 17421-17436, 1989.
- Atwater, T. and J. D. Mudie, Drilled near bottom geophysical study of the Gorda Rise, *J. Geophys. Res.*, 78, 8665-8686, 1973.
- Benerjee, S. K., The magnetic layer of the ocean crust - how thick is it?, *Tectonophysics*, 105, 15-27, 1989.
- Bhattacharyya, B. K., Continuous spectrum of the total magnetic field anomaly due to a rectangular prismatic body, *Geophysics*, XXXI, 97-121, 1966.
- Beske-Diehl, S. J., Magnetization during low-temperature oxidation of seafloor basalts: No large scale chemical remagnetization, *J. Geophys. Res.*, 95, 21413-21432, 1990.
- Bleil, U. and N. Petersen, Variations in magnetization intensity and low-temperature titanomagnetite oxidation of ocean floor basalts, *Nature*, 301, 38388, 1983.
- Bradley, L. M. and H. Frey, Constraints on the crustal nature and tectonic history of the Kerguelen Plateau from comparative magnetic modeling using MASAT data, *Tectonophysics*, 145, 243-251, 1988.
- Cande, S. C., A Paleomagnetic Pole from Late Cretaceous marine magnetic anomalies in the Pacific, *Geophys. J. R. Astron. Soc.*, 44, 547-566, 1986.
- Cande, S. C., J. I. LaBrecque, R. L. Larson, W. C. Pitman, III, X. Goloshenko, and W. Haxby, Magnetic lineations of the world's ocean basins, *Spec. Map, Amer. Assoc. Petr. Geol.*, 1959.
- Carlson, R. L., and C. N. Herrick, Densities and porosities in the oceanic crust and their variations with depth and age, *J. Geophys. Res.*, 95, 91539-91570, 1990.

- Cohen, Y., and J. Achache, New global vector magnetic anomaly maps derived from Magsat data, *J. Geophys. Res.*, 95, 10783-10800, 1990.
- Cohen, Y. and J. Achache, Contribution of induced and remanent magnetization to long-wavelength oceanic magnetic anomalies, *Jour. Geophys. Res.*, 99, 2943-2954, 1994.
- Couill, J.L., Y. Cohen, and J. Achache, The global continent-ocean magnetization contrast, *Earth Planet. Sci. Lett.*, 103, 354-364, 1991.
- Dunlop, D.J., Viscous magnetization of 0.04 -100_m magnetites, *Geophys. J. R. Astron. Soc.*, 74, 667, 1983.
- Engelbreton, D.C., A. Cox, and R.G. Gordon, Relative motions between oceanic and continental plates in the Pacific basin, *Geol. Soc. Amer., Spec. Paper*, 206, 59pp, 1985.
- Fullerton, L.G., H.V. Frey, J. It. Roark, and H.H. Thomas, Evidence for a remanent contribution in Magsat data from the Cretaceous Quiet Zone in the South Atlantic, *Geophys. Res. Lett.*, 16, 1085-1088, 1989.
- Hall, I. M., C. Walls, M. Williamson, B.X. Wang, Depth Trends in magnetic profiles in an area of prolonged cold water drawdown in uppermost Troodos-type oceanic crust., *Can. Jour. Earth Sci.*, Vol 24, p941-952, 1987.
- Hall, J. M., B.E. Fisher, C.C. Wallis, S.J. Hall, H.P. Johnson, A.R. Baker, V. Agrawal, M. Persaud, R.M. Sumaiang, Vertical distribution and alteration of dikes in a profile through the Troodos ophiolite, *Nature*, v. 326, p 780-782, 1987.
- Hall, J.M. and B.E. Fisher. The characteristics and significance of secondary magnetite in a profile through the dike component of the Troodos, Cyprus, ophiolite, *Can. Jour. Earth Sci.*, 24, 2141-2159, 1987.
- Harrison, C.G.A., and H.M. Carle, Intermediate wavelength magnetic anomalies over ocean basins, *J. Geophys. Res.*, 86, 11585-11599, 1981.
- Harrison, C.G.A., Marine magnetic anomalies - the origin of the stripes, *Ann. Rev. Earth Planet. Sci.*, 15, 505-543, 1987.
- Hayling, K.L. and C. G.A. Harrison, Magnetization modeling in the North and equatorial Atlantic Ocean using Magsat data, *J. Geophys. Res.*, 91, 12423-12443, 1986.
- Irving, E., The Mid-Atlantic Ridge near 45 °N, XI V, Oxidation and magnetic properties of basalt: Review and discussion, *Can. Jour. Earth Sci.*, 7, 1528-1538, 1970.
- Johnson, H.P. and T. Atwater, Magnetic study of basalts from the Mid-Atlantic Ridge at 37°N, *Geol. Soc. Amer. Bull.*, 88, 637-647, 1977.
- Kelso, P.R., S.K. Banerjee, H-U. Worn, the effect of Low Temperature Hydrothermal Alteration on the Remanent Magnetization of Synthetic Titanomagnetites: A case for Acquisition of Chemical Remanent Magnetization, *J. Geophys. Res.*, 96, 19545-19553, 1991.
- Kent, D.V., B. Honnorez, N. Opdyke, and P.J. Fox, Magnetic properties of a Red Sea oceanic gabbros and the source of marine magnetic anomalies, *Geophys. J. R. Astron. Soc.*, 55, 513-537, 1978.
- Kikawa, E. and J.E. Pariso, Magnetic Properties of Gabbros from Hole 735B, Southwest Indian ridge, in Von Herzen, R.P., Robinson, P.T., et al., eds., *Proceedings of the Ocean Drilling Program, Scientific Results*, v. 118, 285-307, 1991.
- Klitgord (K.I.), and H. Schouten, Late Kinematics of the Central Atlantic, in *The Geology of North America*, v. M., The Western North Atlantic Region, *Geol. Soc. Amer.*, 351-378, 1989.
- Kusznir, N.J., Thermal evolution of the oceanic crust, its dependence on spreading rate and effect on crustal structure, *Geophys. J. R. Astron. Soc.*, 61, 167-181, 1980.
- LaBrecque, J.L. and P.D. Rabinowitz, Magnetic Anomalies - Argentine Continental Margin, Argentine Basin, North Scotia Ridge, Falkland Plateau, *Amer. Assoc. Petr. Geol., Special Map Series*, Cat. No. 826, 197-i.
- LaBrecque, J. L. and S.C. Cande, Intermediate-wavelength magnetic anomalies over the central Pacific, *J. Geophys. Res.*, 89, 11124-11134, 1984.

- LaBrecque, J.L., S.C. Cande, R.D. Jarrard, Intermediate wavelength magnetic anomaly field of the North Pacific and possible source distribution, *J. Geophys. Res.*, 90, 2549-2564, 1985.
- LaBrecque, J.L., and C.A. Raymond, Seafloor spreading anomalies in the Magsat field of the North Atlantic, *J. Geophys. Res.*, 90, 2565-2575, 1985.
- Langel, R.A. and R. H. Estes, A geomagnetic field spectrum, *Geophys. Res. Lett.*, 9, 250-253, 1982.
- Langel, R. A., J.D. Phillips, and R.J. Homer, Initial Scalar magnetic anomaly map from Magsat, *Geophys. Res. Lett.*, 9, 269-272, 1982.
- Larson, R.I. and C.G. Chase, Late Mesozoic evolution of the western Pacific Ocean, *Geol. Soc. Am. Bull.*, 83, 3627-3644, 1972.
- Lasaga, A. C., Rate laws of chemical reactions, Kinetics of Geochemical Processes, edited by A.C. Lasaga and R.J. Kirkpatrick, *Rev. Mineral.*, 8, 1-68, 1981.
- Macdonald, K.C., Near bottom magnetic anomalies, asymmetric Spreading, oblique spreading and tectonics of the Mid-Atlantic Ridge near 37°N, *Geol. Soc. Am. Bull.*, 88, 541-555, 1977.
- Macdonald, K.C., A geophysical comparison between fast and slow spreading center: Constraints on magma chamber formation and hydrothermal activity, in *Hydrothermal Processes at Seafloor Spreading Centers*, Rona, Boston, Larber, Smith eds., Plenum Press, N. Y., 27-51, 1983.
- Mayhew, M. A., Curie Isotherm Surfaces Inferred from High-Altitude Magnetic Anomaly Data, *Jour. Geophys. Res.*, 90, 2647-2654, 1985.
- McKenzie, D.P., Some remarks on heat flow and gravity anomalies, *J. Geophys. Res.*, 72, 6261-6273, 1967.
- Merrill, R.T. and M.W. McElhinney, *The Earth's Magnetic Field*, London, Academic Press, 401pp, 1983.
- Morgan, W. J., Hot spot tracks and the opening of the Atlantic and Indian Oceans, in Emiliani, C. ed., *The Sea*, v. 7, New York, Wiley Interscience, 433-487, 1981.
- Pal, P.C. and P.H. Roberts, Long-term polarity stability and strength of the geomagnetic dipole, *Nature*, 331, 702-705, 1988.
- Parker, R. I. and D.W. Oldenburg, Thermal model of ocean ridges, *Nature, Phy. Sci. Lond.*, 242, 137-139, 1973.
- Paraiso, J.E. and Johnson, H.I., Alteration Processes at Deep Sea Drilling Project / Ocean Drilling Program Hole 504B at the Costa Rica Rift: Implications for Magnetization of Oceanic Crust, *J. Geophys. Res.*, 96, 11703-11722, 1991.
- Pitman, W.C. III, E.M. Herron, and J.R. Heirtzler, Magnetic Anomalies in the Pacific and Sea Floor Spreading, *J. Geophys. Res.*, 73, 2069-2085, 1968.
- Pitman, W.C. III and M. Talwani, Sea Floor Spreading in the North Atlantic, *Geol. Soc. Am. Bull.*, 83, 619-646, 1972.
- Pluoff, J., Gravity and Magnetic Field of Polygonal Prisms and Application to Magnetic Terrain Corrections, *Geophysics*, 41, 727-741, 1976.
- Raymond, C.A., and J. L. LaBrecque, Magnetization of the oceanic crust: thermomagnetic magnetization or chemical remnant magnetization, *J. Geophys. Res.*, 92, 8077-8088, 1987.
- Sailor, R. V., A.R. Lazarewicz, and R.F. Brammer, Spatial Resolution of Magsat crustal anomaly data over the Indian Ocean, *Geophys. Res. Lett.*, 9, 289-292, 1982.
- Shive, P.N., R. Frost, A. Peretti, The magnetic properties of metaperidotitic rocks as a function of metamorphic grade: Implications for crustal magnetic anomalies, *J. Geophys. Res.*, 93, 12187-12195, 1988.
- Shure, L. and R.I. Parker, An alternative explanation for intermediate-wavelength magnetic anomalies, *J. Geophys. Res.*, 86, 11600-11608, 1981.
- Smith, G. and Banerjee, S.K., Magnetic Structure of the Upper Kilometer of the Marine Crust at Deep Sea Drilling Project Hole

- 504B, Eastern Pacific Ocean, *J. Geophys. Res.*, **91**, 10337-10354, 1986.
- Swift, B.A. and H.L. Johnson, Magnetic properties of the mafic dykes of the Ophiolite suite and implications for the magnetization of oceanic crust, *J. Geophys. Res.*, **89**, 3291-3308, 1984.
- Tivey, M.A. and H.L. Johnson, The Central Anomaly magnetic high: Implications for ocean crust construction and evolution, *J. Geophys. Res.*, **92**, 12,655-12,695, 1987.
- Tucholke, B.E. and F.W. McCoy, Paleogeographic and paleobathymetric evolution of the North Atlantic Ocean, in *The Geology of North America*, v. M, The Western North Atlantic Region, Chapter 325, *Geol. Soc. Amer.*, 589-602, 1986.
- Toft, P. B. and J. Arkani-Hamed, Magnetization of the Pacific Ocean Lithosphere Deduced from Magsat Data, *Jour. Geophys. Res.*, **97**, 4387-4406, 1992.
- Vera E.E., J.C. Mutter, P. Buhl, J.A. Orcutt, A.J. Harding, M. E. Kappus, R.S. Detrick, T.M. Brocher, The structure of 0- to 0.2 My. -old oceanic crust at 9 N on the East Pacific Rise from expanded spread profiles, *J. Geophys. Res.* **95**, 15529- 15656, 1990.
- Vine, J.J. and D.H. Matthews, Magnetic anomalies over Oceanic ridges, *Nature*, 199, 947-949, 1963.
- Vogt, P.R. and A.M. Einwich, Magnetic anomalies and seafloor spreading in the western North Atlantic and a revised calibration of the Keathly M geomagnetic reversal chronology, *Initial Reports of the Deep Sea Drilling Project*, **93**, 857-876, 1979.
- Vogt, P.R., Magnetic anomalies and crustal magnetization in The Geology of North America, v. M., The Western North Atlantic Region, *Geol. Soc. Amer.*, 229-255, 1986.
- Wasilewski, P.J., H.L. Thomas, M.A. Mayhew, The Moho as a Magnetic Boundary, *Geophys. Res. Lett.*, **6**, 541-544, 1979.
- Weissel, J.R., and D.E. Hayes, Magnetic anomalies in the southeast Indian Ocean, in *Antarctic Oceanology II*, In: *The Australian-New Zealand sector*, *Antarct. Res. Ser.*, **19**, 165-169, Washington, D.C., AGU, 1972.
- White R.S., R.S. Detrick, J. C. Mutter, P. Buhl, T.A. Minshull, E. Morris, New Seismic images of oceanic crust structure, *Geology*, **18**, 462-465, 1990.
- Winterer, E.L., Sediment thickness map of the northeast Pacific, in *The Geology of North America*, v. N, The Eastern Pacific Ocean and Hawaii, Chapter 14, *Geol. Soc. Amer.*, 307-310, 1989.

Gonzalo A. Yañez, SERNAGEOMIN, Casilla 10465,
Santiago, Chile, (e-mail: goyanez@ccc.uchile.cl).

J.L. Labrecque, Code YSG, NASA, Washington, DC 20037,
(e-mail: jlabrecq@mtpe.hq.nasa.gov).

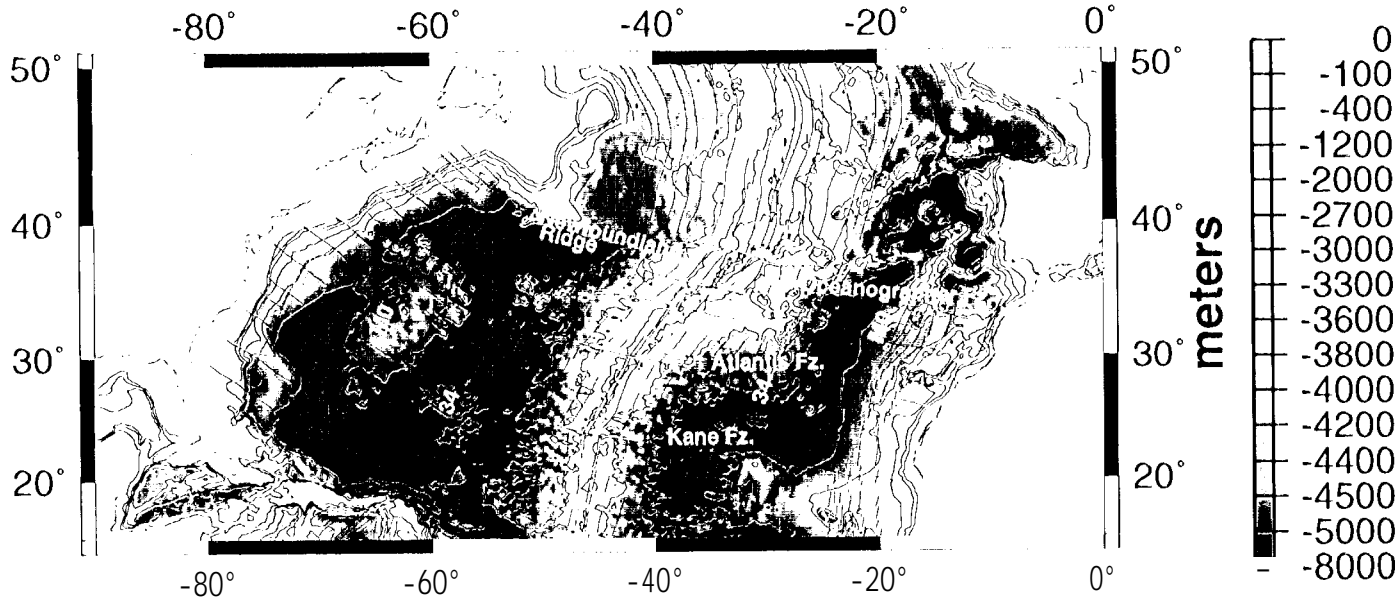
(Received March 12, 1996; accepted March 19, 1996.)

¹ Also at the Lamont-Doherty Earth Observatory of Columbia University

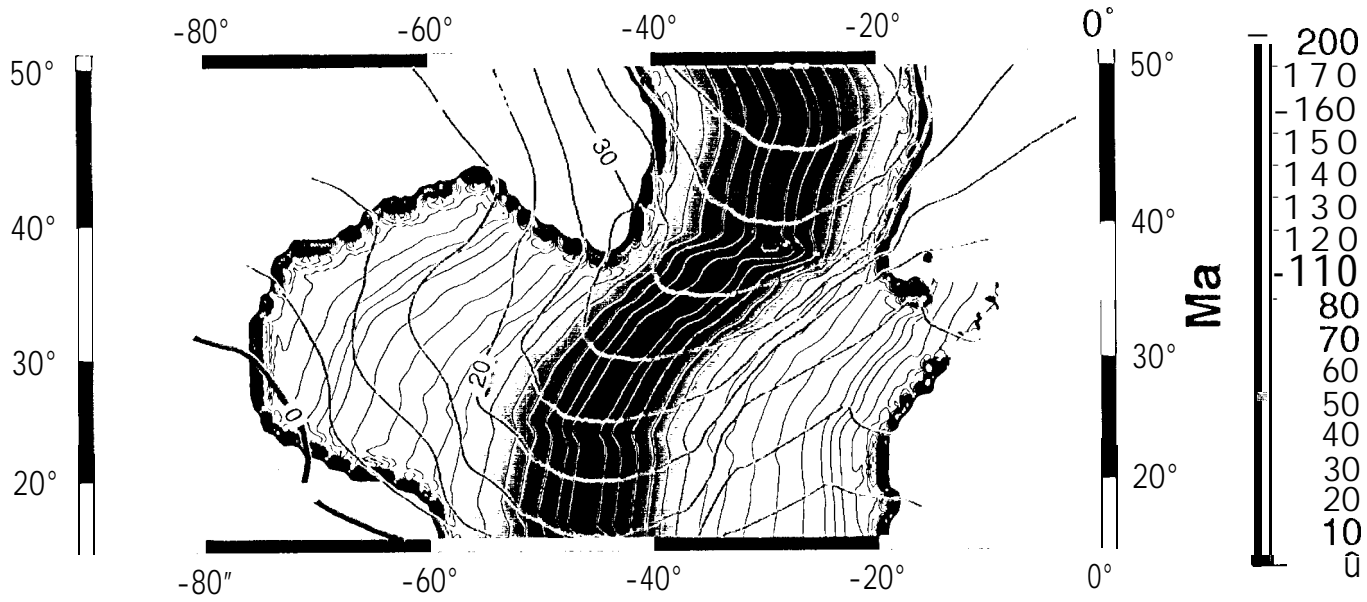
Copyright 1996 by the American Geophysical Union

Paper number JB9601-64.
0148-0227/96/96JB-00164\$05.00

a. Tectonic Map



b. Age & Paleo Incl.



c. Magsat

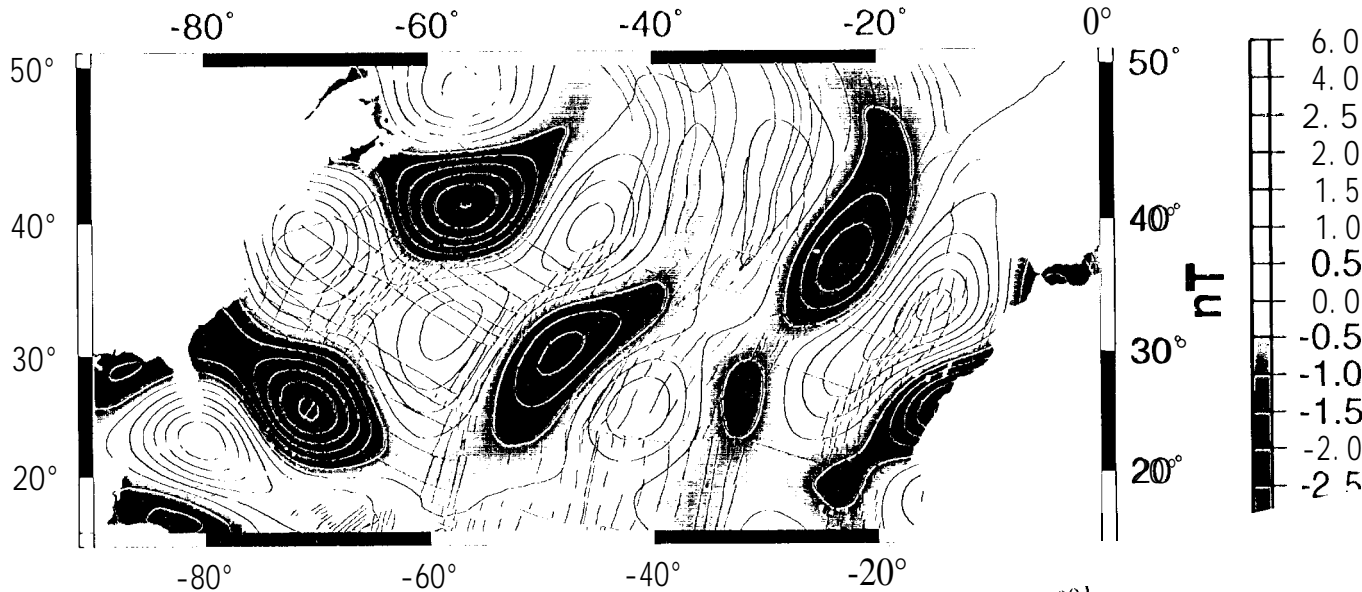
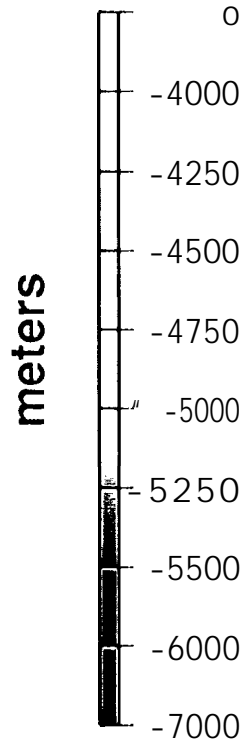
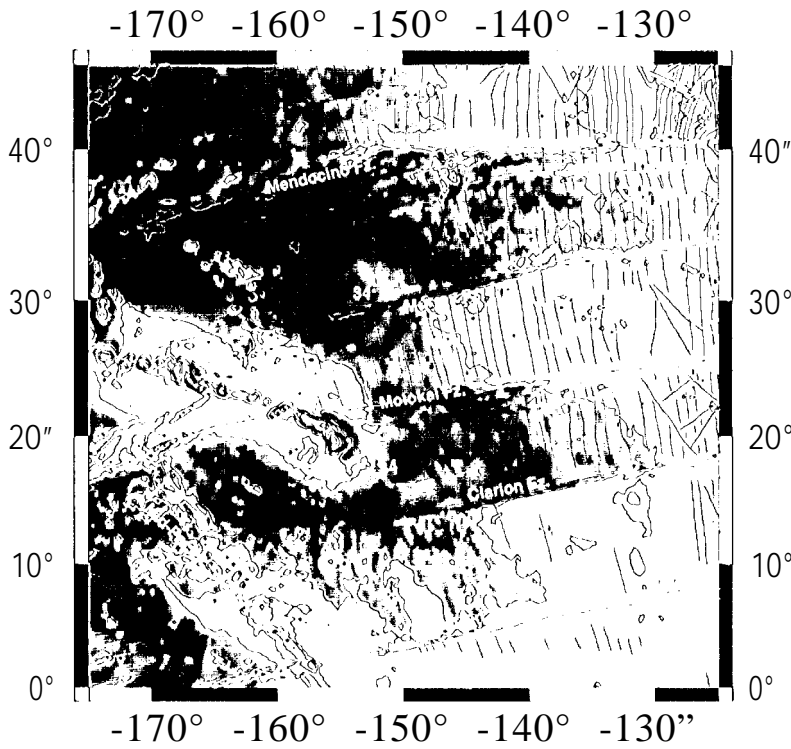
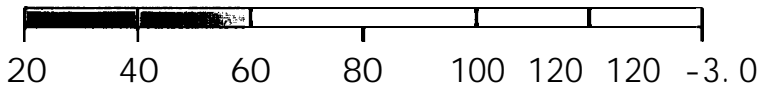
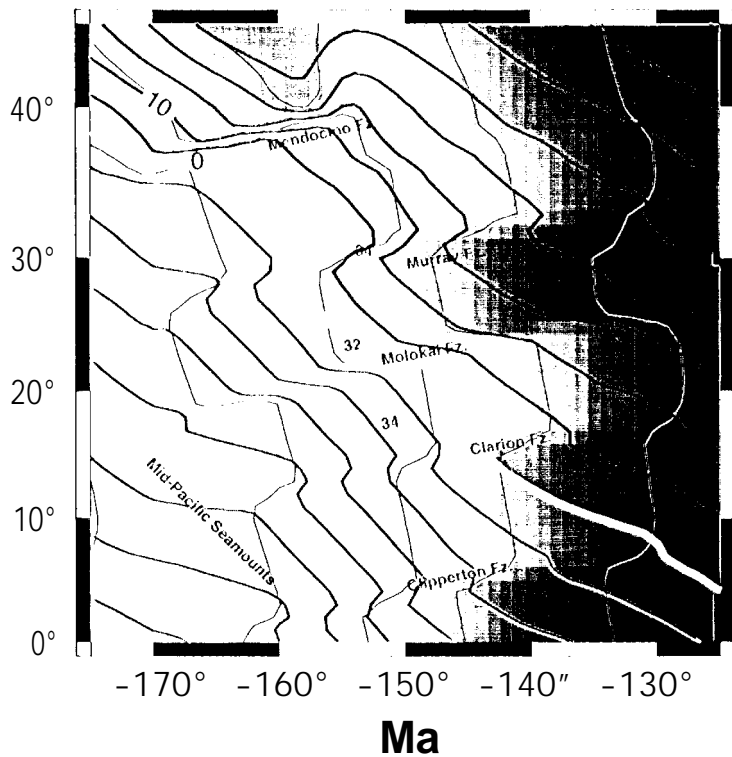


Figure 1. North Atlantic: a. Tectonic map fracture zones and magnetic lineations from Cancian et al [1989] in red superimposed on color coded bathymetry; b. Oceanic Age (in colors) and Paleo-latitude of each block; c. Magsat magnetic field intensity in the North Atlantic hemisphere.

a. Tectonic Map



b. Age & Paleo Incl.



c. Magsat

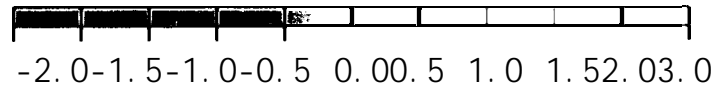
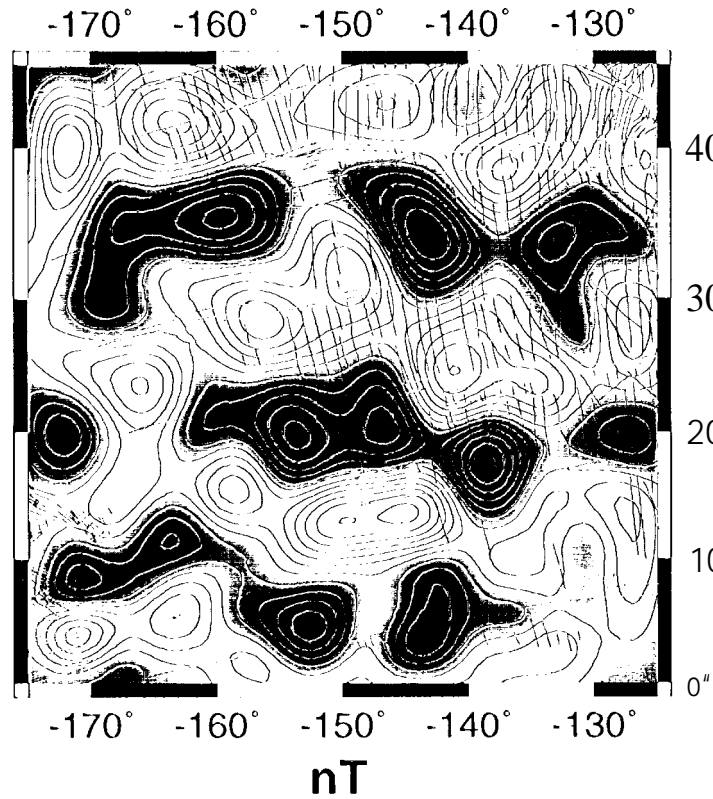


Figure 2. Northeast Pacific same nomenclature as Figure 1): a. Tectonic map; b. Oceanic Age and Paleomagnetic Inclination; c. Magsat field from Arkani-Hamed and Strangway [1985].

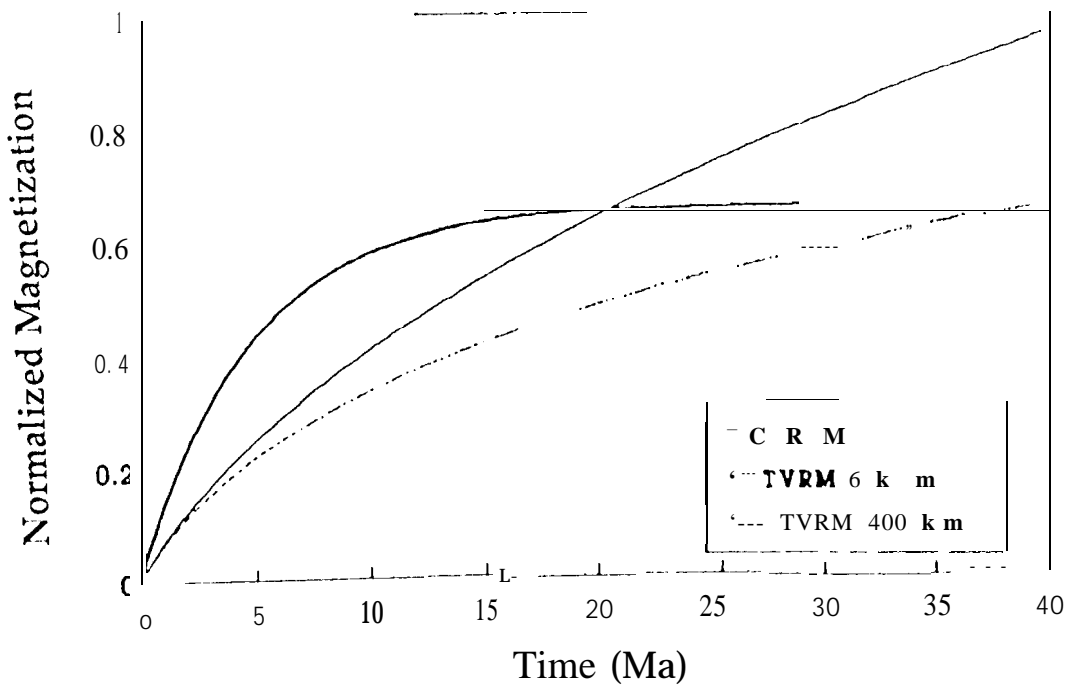
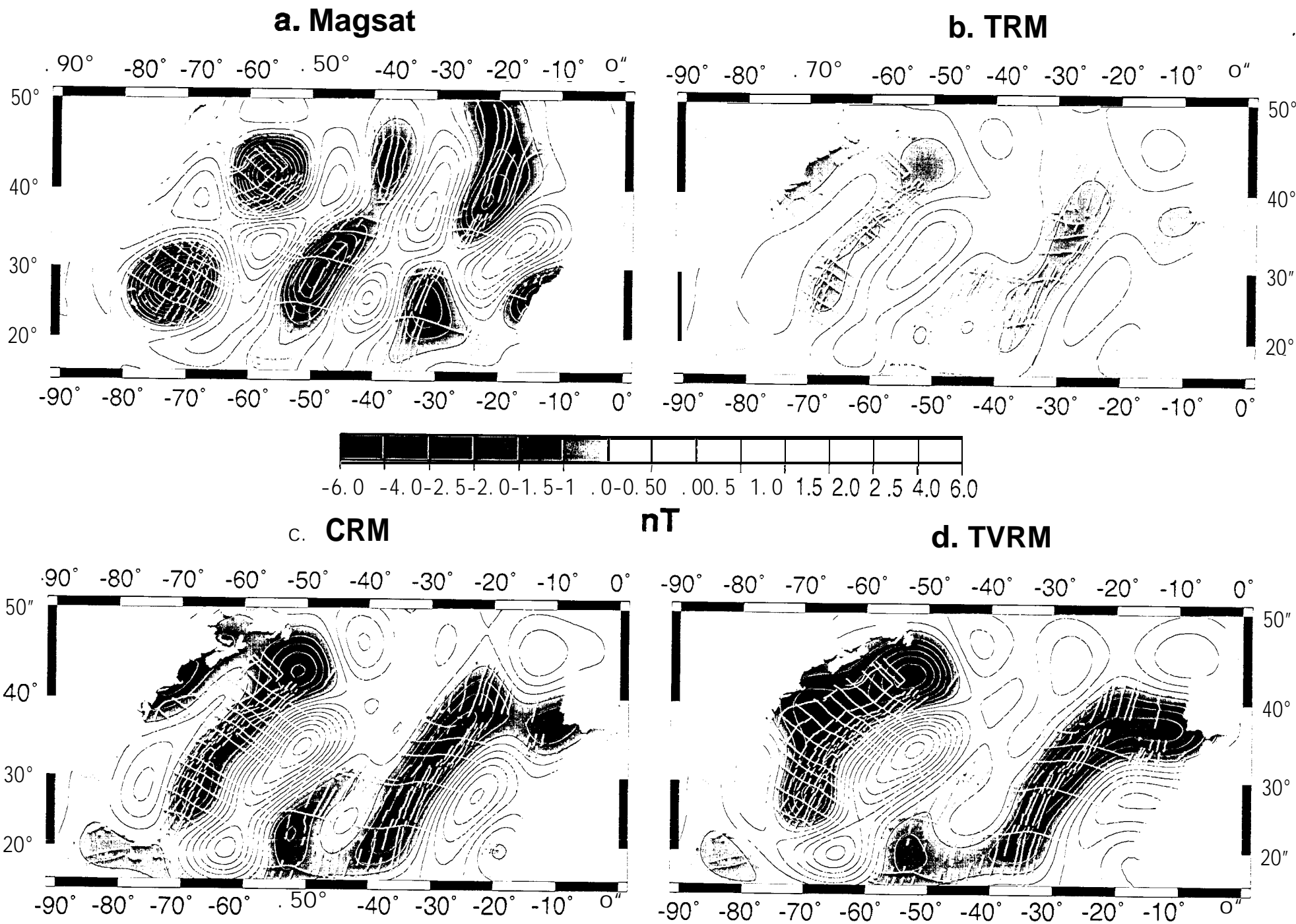
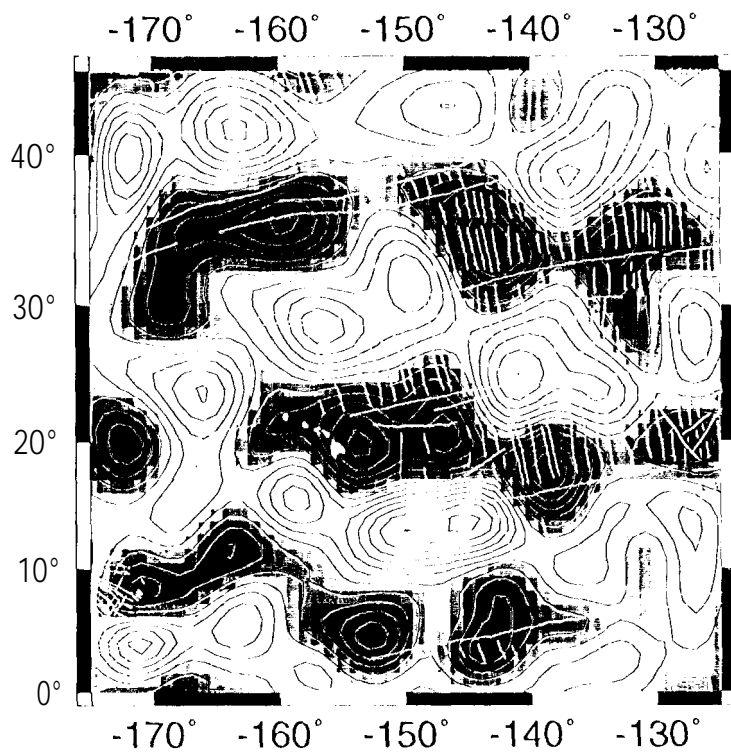


Figure 3. Secondary magnetic acquisition within a normal magnetic polarity interval, CRM: heavy line, TVRM at Magsat altitude (400 km): clotted line, TVRM at sea surface: segmented line. The units of the vertical axis are normalized.

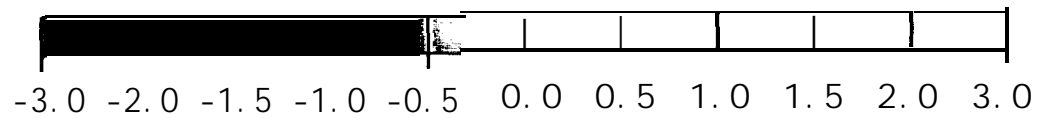
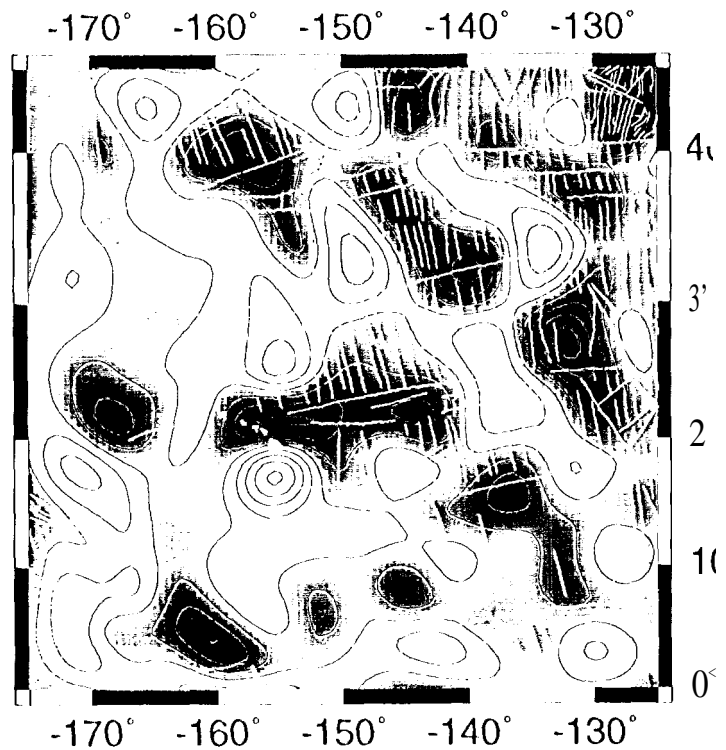
Figure 4. North Atlantic 3-D magnetic modeling: a. Magsat data, b. TRM; c. CRM; d. TVRM; contour lines at 0.5 nT interval.



a. MAGSAT

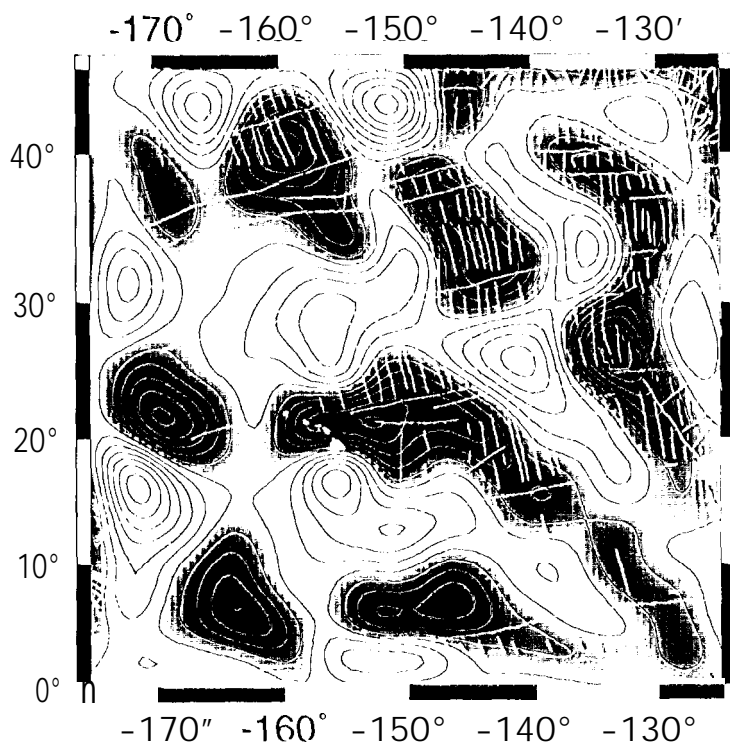


b. TRM



nT

c. CRM



d. TVRM

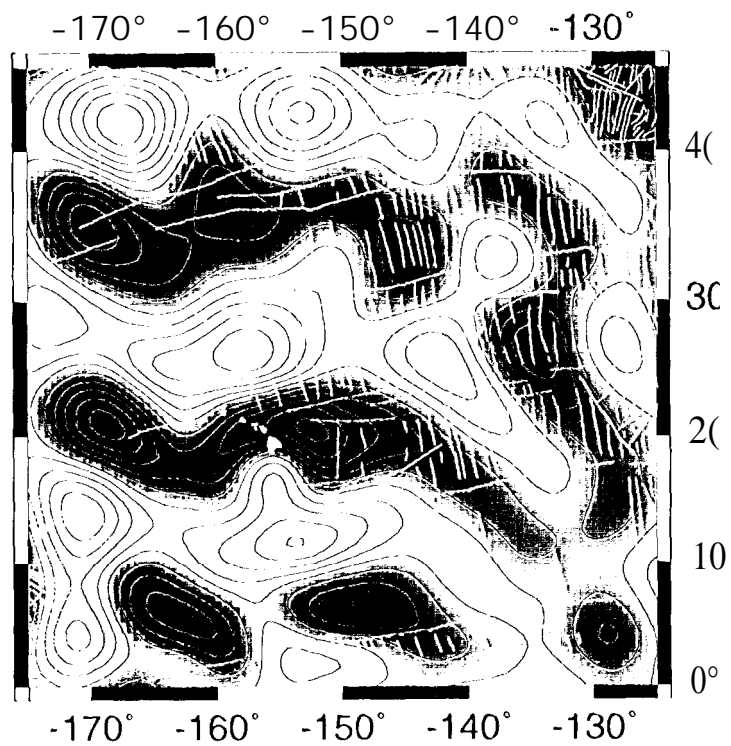
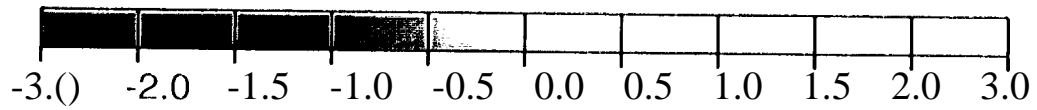
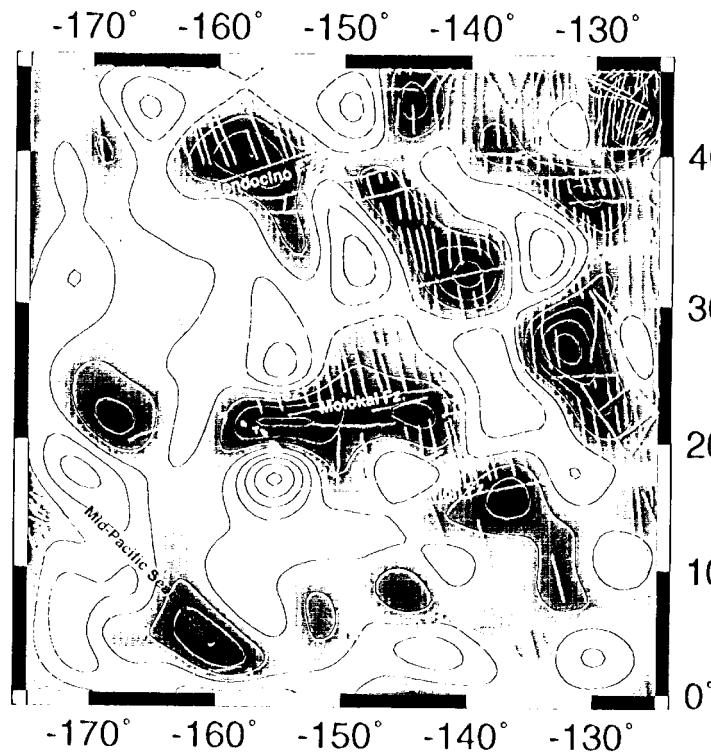
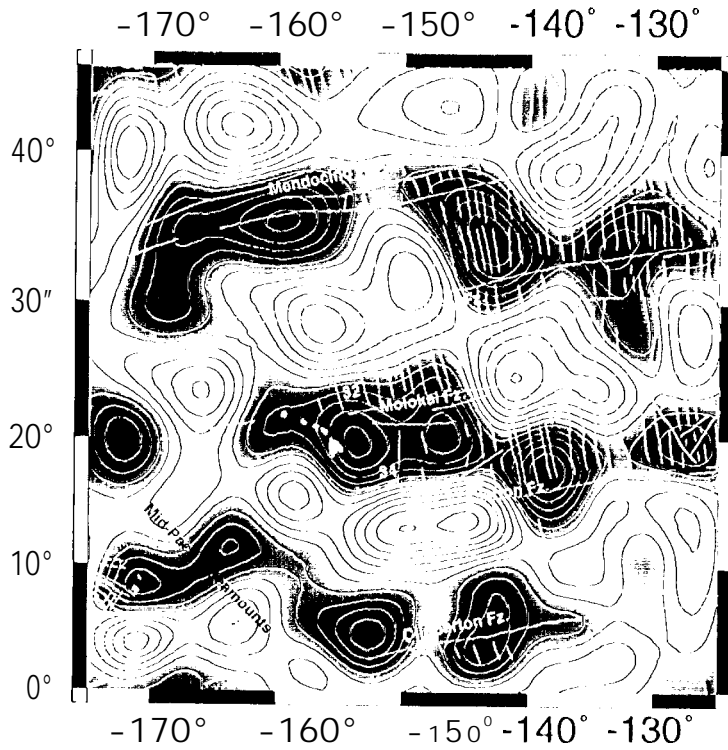


Figure S. Northeast Pacific 3-D magnetic modeling: a. Magsat data; b. TRM; c. CRM; d. TVRM; contour lines at 0.5 nT interval.

a. MAGSAT

b. TRM



c. CRM

nT

d. TVRM

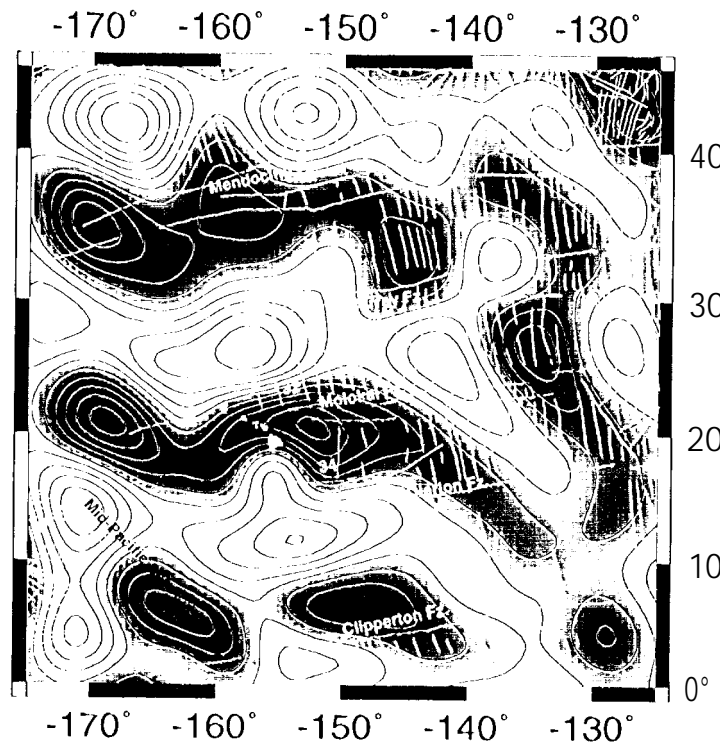
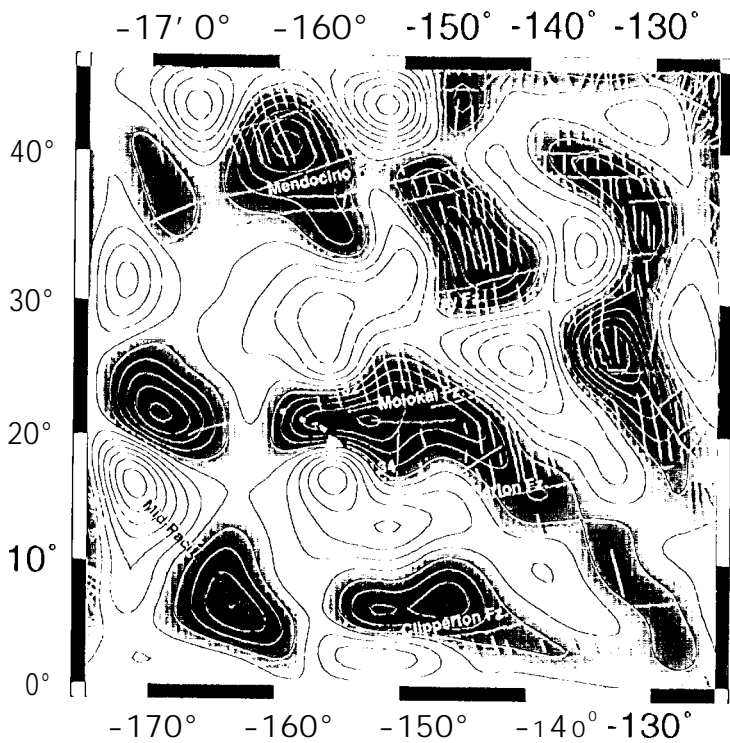


Figure 6. Northeast Pacific: a. Sea surface magnetic field compiled following the technique described in LaBrecque et al. [1985]. b. Age map contour lines: 10